OPTIMIZATION OF METAL FORMING PROCESSES FOR IMPROVING FINAL MECHANICAL STRENGTH

J.-L. CHENOT[*], P.-O. BOUCHARD[*], L. FOURMENT[*], P. LASNE[†] AND E. ROUX[*]

[*] CEMEF – Mines Paristech, UMR CNRS n° 7635
BP 207 – 06904 Sophia Antipolis Cedex, France
e-mail: Jean-loup.chenot@mines-paristech.fr, web page: http://www.cemef.mines-paristech.fr/

[†] Transvalor S.A., Parc de Haute Technologie, Sophia Antipolis , 694, av. du Dr. Maurice Donat
06255 Mougins Cedex, France
Email: patrice.lasne@transvalor.com - Web page: http://www.transvalor.com/index_gb.php

Key words: Metal forming, Finite element, Optimization, Identification, Mechanical properties.

Abstract.

The fundamental mechanical assumptions and the basic principles of 3-dimensional FE discretization are briefly summarized. Several important numerical developments for efficient and accurate computation of large plastic deformation are discussed. Material behavior must be known precisely: material parameters of the constitutive law, thermal law and friction law must be determined by experimental tests and identification procedures by inverse modeling. Is it also necessary to avoid the possible onset of defects, such as crack opening, by introducing damage modeling in the cost function. A parameter sensitivity analysis is utilized in order to select the most important factors: shape of the preform, tools geometry, etc. The practical optimization is carried out by a genetic algorithm technique or by a surface response method. Moreover, for assessing the fatigue behavior, a more local approach is necessary in order to take into account material evolution at the micro scale.

1 INTRODUCTION

Optimization of industrial forming processes has received a growing attention to increase competitiveness. Until recently this objective was the result of a long and expensive procedure, mostly achieved by trial and error, using industrial equipments and real materials. Finite element simulation of metal forming processes started in the 70's for 2D problems [1-4] and in the 80's for 3D configurations [5]. To-day commercial simulation codes facilitate trial and error optimization. However, in view of the continuous improvement of softwares and computing facilities, including parallel computing, it is now possible to consider *automatic optimization*, where the optimal solution is mostly found by computation.

A software, called MOOPI (MOdular software dedicated to Optimization and Parameters Identification) has been developed in CEMEF to address these issues. MOOPI, presented in Figure 1, is based on 4 different layers. The basic layer 0 represents the direct model, which is the finite element computation Forge in our case. Layer 1 deals with sensitivity analyses and enables us to check the influence of input parameters on output observables. Layer 2 is the optimization layer in order to find optimal parameters of any kind of numerical simulations. Finally layer 3 deals with inverse analysis for automatic materials parameters analysis by comparing experimental and numerical observables. Each layer can use the algorithms implemented in the other layers. For example, inverse analysis uses the optimization algorithms developed in the second layer in order to minimize the cost function, defined as the sum of the squared differences between experimental and numerical observables. If response surfaces are needed in the optimization algorithm, the sensitivity analysis layer can also be used to give the initial database using DoE (Design of Experiment) techniques.
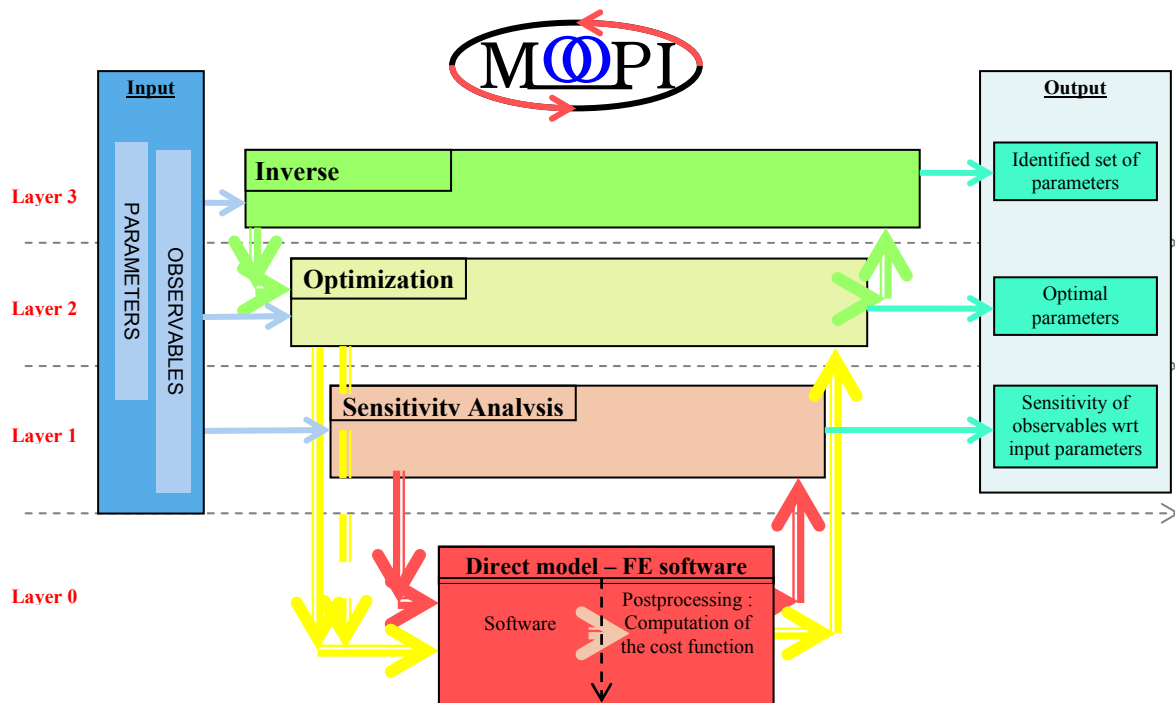

Figure 1 : Flowchart of the MOOPI software

2 MECHANICAL AND NUMERICAL APPROACH

The finite element approach of metal forming processes was described in [6], to which the interested reader is referred for more details.

2.1 – Mechanical and Thermal Description

Introducing an additive decomposition of the strain rate tensor $\dot{\varepsilon}$ into an elastic part $\dot{\varepsilon}^e$ and a plastic (or viscoplastic) one $\dot{\varepsilon}^p$:

$$\dot{\varepsilon} = \dot{\varepsilon}^e + \dot{\varepsilon}^p \tag{1}$$

Utilizing the Jauman objective derivative of the stress tensor , the hypo elastic law is written:

$$\frac{d\sigma_J}{dt} = \lambda^e \text{trace}(\dot{\varepsilon}^e)I + 2\mu^e \dot{\varepsilon}^e \tag{2}$$

where λ^e and μ^e are the Lamé coefficients. The plastic or viscoplastic component of the strain rate tensor obeys a general Perzyna rule of the form:

$$\dot{\varepsilon}^p = 3/2\sigma_{eq} \left\langle (\sigma_{eq} - R)/K \right\rangle^{1/m} \sigma' \tag{3}$$

where σ_{eq} is the equivalent strain, σ' is the deviatoric stress tensor, $\dot{\bar{\varepsilon}}$ is the equivalent strain rate and $\bar{\varepsilon}$ is the equivalent strain, K, R and m are material parameters.

At the interface between part and tool, the friction shear stress can be modeled by a "viscoplastic Coulomb" law, in term of the normal stress σ_n and the tangential velocity Δv :

$$\tau = -\alpha_f |\sigma_n| \Delta v / |\Delta v|^{1-p} \tag{4}$$

Where α_f and p are friction coefficients.

For a quasi incompressible material flow, a mixed formulation in term of velocity v and pressure p is chosen in the domain Ω; for any virtual velocity and pressure fields v^*, p^* :

$$\int_\Omega \sigma' : \dot{\varepsilon}^* \, dV - \int_\Omega p \, \text{div}(v^*) dV - \int_{\partial\Omega_c} \tau v^* \, dS = 0 \tag{5}$$

Introducing the material compressibility κ, the mass conservation equation is written:

$$-\int_\Omega (\kappa \text{div}(v) + \dot{p}) p^* dV = 0 \tag{6}$$

The total time of the process is decomposed into small increments Δt, and the displacement field is assumed to be proportional to the velocity field at the beginning of the increment:

$$\Delta u = \Delta t \, v \tag{7}$$

In the same way the stress increments are introduced, so that eqs. (5) and (6) are rewritten:

$$\int_\Omega (\sigma' + \Delta\sigma') : \dot{\varepsilon}^* \, dV - \int_\Omega (p + \Delta p) \text{div}(v^*) dV - \int_{\partial\Omega_c} \tau v^* \, dS = 0 \tag{8}$$

$$-\int_\Omega (p\Delta t / \kappa + \text{div}(\Delta u)) : p^* \, dV = 0 \tag{9}$$

For hot forming process the heat equation is introduced:

$$\rho c \, dT / dt - \text{div}(k \, \text{grad}(T)) - r\sigma : \dot{\varepsilon} = 0 \tag{10}$$

Where ρ is the material density, c the heat capacity, k the thermal conductivity and r the fraction of plastic work transformed into heat. The thermal and mechanical coupling originates from heat generation by plastic work, thermal dilatation which modifies eq. (9), and the dependency of the material parameters on temperature, e.g.:

$$K = K_0 \left(\varepsilon_0 + \overline{\varepsilon}\right)^n \exp(\beta / T), \; m = m_0 + m_1 T \tag{11}$$

2.2 – Finite Element Discretization

To achieve robustness and compatibility with other numerical requirements, a mixed displacement (or velocity) and pressure formulation with P1+P1 stabilized elements is chosen. The pressure field is discretized using tetrahedral elements with 4 linear shape functions M_n, while the velocity, or the displacement field, uses 5 shape functions N_n: the linear functions plus a bubble function. The discretized mixed integral formulation for the mechanical problem is:

$$R_n^U = \int_\Omega (\sigma' + \Delta\sigma') : \mathbf{B}_n dV - \int_\Omega (p + \Delta p)\, \text{trace}(B_n)\, dV + \int_{\partial\Omega_c} \alpha_f \left|\sigma_n\right| \frac{\Delta v}{\left|\Delta v\right|} N_n dS = 0 \tag{12}$$

$$R_m^P = \int_\Omega (\frac{\kappa}{\Delta t} div(\Delta u) + p) M_m dV = 0 \tag{13}$$

To which the discretized heat equation is added:

$$\mathbf{C}.\Delta\,\mathbf{T} + \mathbf{H}'.\mathbf{T}\,\Delta t + \mathbf{F}\,\Delta t = 0 \tag{14}$$

Where **C** is the heat capacity matrix, **H'** is the conduction matrix and **F** is a vector gathering the boundary conditions and the heat source terms. Equations (12) and (13) on one hand and equation (14) on the other hand can be solved separately until convergence or using a global Newton Raphson algorithm.

2.3 - Numerical problems

2.2.1 Remeshing
Remeshing steps are compulsory when deformation of the work-piece results in too distorted elements and when contact occurs progressively between tools and the part. An iterative method is designed to remesh locally where it is necessary. Moreover, for a more reliable control of accuracy, an estimation of the discretization error is performed and the elements must be refined locally in the zones where the strain is higher. This is achieved by prescribing a local size of the elements and rebuilding the mesh accordingly [7]. But this approach may lead to generate a very large number of elements. This drawback can be partly overcome, by introducing anisotropic meshes having narrow elements in the direction of high strain gradient and elongated ones in the orthogonal direction [8].

2.2.2 Equations Solving
At each time increment several linear systems are generated by the Newton-Raphson procedure, their resolutions representing the more expensive contribution to the total CPU

time. Iterative methods are effective on the reasonably well conditioned systems we get due to the stabilization induced by the choice of $P1^+P1$ elements. These methods can be parallelized, provided a domain partitioning is defined, each sub domain being treated on a separate processor [8].

2.2.3 Multi Material Coupling

The problem of multi material coupling appears when the tools are considered as elastically deformable, or when a part is formed with several materials. At the interface between different materials, we must impose a unilateral contact condition with friction (and possibly with a force of cohesion). However challenging numerical problems appear to take into account this situation with non coincident meshes at the interface between materials. In the "master and slave approach", a Lagrange multiplier contribution of the non linear equations to solve is introduced to avoid penetration of the slave surface $\partial\Omega_B^{contact}$, into the master surface $\partial\Omega_A^{contact}$. But this approach is effective only when the surface mesh of the slave is more refined than the surface mesh of the master in contact. A quasi symmetric Lagrange multiplier formulation, was proposed by Fourment et al in [9] in which the additional term is written:

$$\Lambda^{QSYM} = \frac{1}{2}\left(\int_{\partial\Omega_B^{contact}} h_A(\Delta u_B)\lambda^B ds_B + \int_{\partial\Omega_A^{contact}} h_B(\Delta u_A)\overline{\lambda}^B ds_A \right) \tag{15}$$

Where λ^A is the Lagrange multiplier defined on $\partial\Omega_A^{contact}$ and $\overline{\lambda}^B$ is the projection of λ^B on the surface $\partial\Omega_A^{contact}$. With a nodal formulation, the quasi symmetric approach imposes a number of constraints equal to the number of nodes of the slave mesh in contact. This method was applied successfully to forging with deformable tools.

2.2.4 Multi grid and multi mesh.

A major concern in numerical simulation is to reduce CPU time in order to be able to solve more complex problems, involving more refined meshes. However the CPU time is not a linear function of the number of unknowns, even for iterative solvers. The multi grid method is a way to achieve a quasi linear dependence of resolution time and consequently to reduce dramatically the computational cost. In ref. [10] a promising node-nested Galerkin multigrid method is described for solving very large linear systems originating from linearization of 3D metal forming problems. The smoothing and coarsening operators are built, using node-nested meshes made of unstructured tetrahedra. The coarse meshes are built by an automatic coarsening algorithm based on node removal and local topological remeshing techniques. A research version of the Forge finite element software was utilized to test the effectiveness of the multigrid solver, for several large scale industrial forging problems and it was shown that the decrease of CPU time can reach a factor higher than 7.

Another method for saving computational cost is to utilize different meshes as developed in ref. [11]. In hot incremental forming, such as cogging or ring rolling, a unique mesh for mechanical and thermal simulation is not the optimal choice. A Bimesh method will use different finite element meshes for the resolution of the different physical problems:

- a main fine mesh to store the results and to carry out the linear thermal computations with one unknown per node,
- a less refined mesh for the non-linear mechanical calculations with 4 unknowns per node.

The numerical development of the Bimesh method consists mainly in building the embedded meshes and managing the data transfer between the meshes. The Bimesh method leads to a CPU reduction of about 4 on industrial examples and is compatible with parallel calculations.

2.2.5 Finite Element modeling at the micro scale

It is well known that the micro (or nano) structure of metals is a key factor for determining the constitutive law during forming and for predicting the final properties of the work-piece. To treat in an average way, the evolution of the material micro structure during thermal and mechanical treatments, the classical method is based on a macro description, selecting representative material parameters (grain size, phase percentage, precipitates, etc.) and to identify physical laws which govern the evolution of these parameters, and their influence on the mechanical behavior [12]. The macro approach is quite convenient for coupling thermal, mechanical and physical computation, but it suffers severe limitations and needs a large amount of experiments to identify the physical laws describing micro structure evolution. On the other hand, computation at the micro scale is now possible and is developed for a more realistic description of materials. Micro modeling is potentially much more accurate but, due to heavier computer cost at the local micro level, direct coupling with macro thermal and mechanical simulations seems limited to 2D problems and simple parts, even with large clusters of computers. One way to view the middle term applications is to use micro modeling of material in post processing, to predict micro structure evolution for a limited number of locations in the work piece, neglecting coupling effects. Another method is to utilize the micro approach to help identification of macro laws. The basic ingredients of the general micro model developed at CEMEF are summarized in [13].

3 INVERSE METHOD FOR MATERIAL PARAMETERS IDENTIFICATION

For a given material law, inverse analysis is used to determine the best parameters that fit experimental data. Identification of the parameters is achieved by minimizing a least square cost function which evaluates the difference between computed and experimental values. In the past differentiation methods were mostly utilized [14], but for a more general approach it was realized that optimization methods using only the evaluation of the least square function must be preferred.

A parallel optimization algorithm based on EGO (Efficient Global Optimization Algorithm) suggested by Jones et al. [15], has been developed for identification and integrated in the MOOPI software. A flowchart of this algorithm is presented in Figure 2. The main idea of this extension is the following: instead of evaluating exactly the cost function of one new set of parameters at each iteration, the idea is to temporally set the cost function value to an approximate value regarding the kriging meta-model. This temporally approximation of the cost function value is not time consuming and enables to extract a new set of parameters from the meta-model without exact evaluation. N set of parameters can thus be extracted from the meta-model without any exact evaluation. The final step is to evaluate exactly the cost function value of these N new points, which can be done simultaneously using parallel computing.

The EGO algorithm implemented in MOOPI is well suited for parameters identification by inverse analysis. This software is able to work with multiple experimental observables and

multiple mechanical tests. The optimization procedure gives the set of identified parameters. Another useful information is a map of the objective function all over the parameters design space. This map is particularly interesting to understand the sensitivity of the observable regarding each parameter of the model.
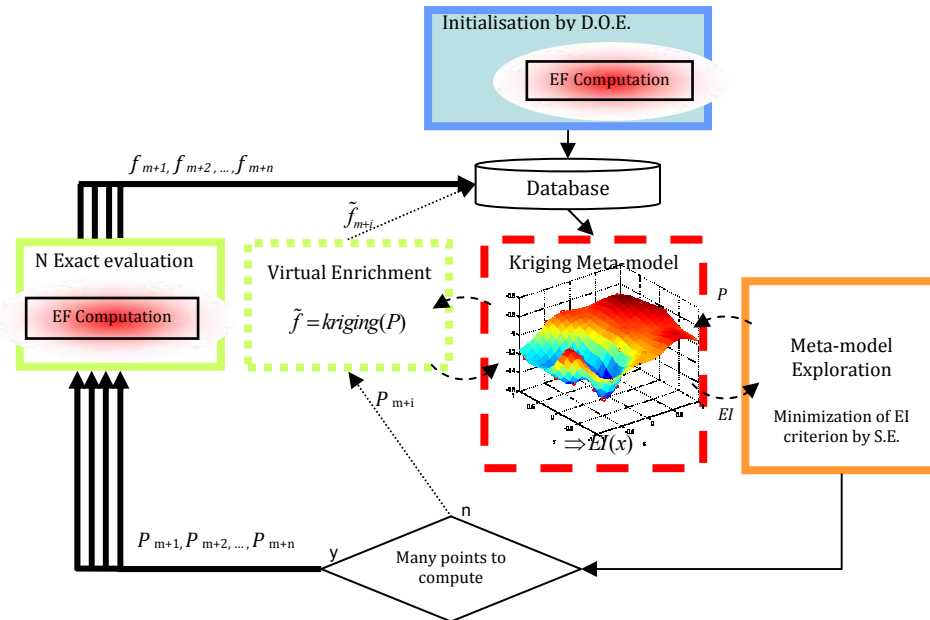

Figure 2: Flowchart of the parallel extension of the EGO algorithm implemented in the MOOPI software

As an example, we identified both elastic-plastic materials behavior law and Lemaître ductile damage parameters, in order to study the final mechanical strength of the clinched component. Figure 3 shows the identified and experimental load-displacement curves, and necking-displacement curves.
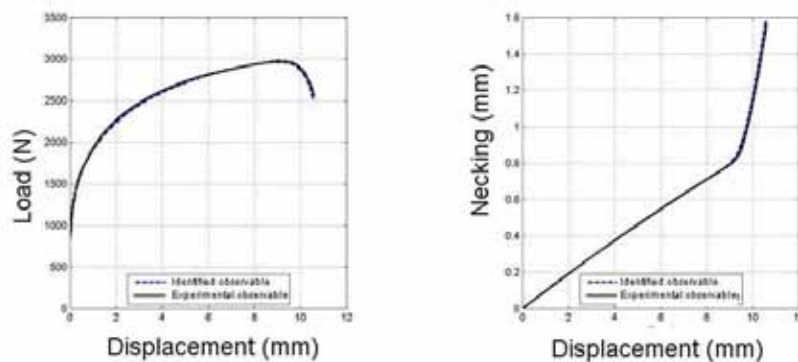

Figure 3: Identified and experimental load-displacement and necking-displacement curves

4 SENSITIVITY ANALYSIS

For any kind of manufacturing processes, input data are always subjected to variability or uncertainty. These variability issues can be experimental (prescribed load, temperature, lubrication, exact materials behaviour, friction, etc.) or numerical (mesh size, time step, etc.). Sensitivity analysis studies are essential to evaluate the impact of input data variability on output results and possibly to select the more important parameters for optimization. In our MOOPI software, finite element computations can be run iteratively with different input data. Observables are stored and compared to check the influence of input data on final results. The modification of input parameters can be done manually by the user, or can be obtained through a Design of Experiments (DoE). Sensitivity analysis is applied here to the study of the clinching process, where a sheet is deformed by the tools illustrated in Figure 4a. The idea is to find the clinching process parameters that have the highest influence on the final mechanical strength of the joined component. A sensitivity analysis has been done on the punch and lower die geometries, as shown in Figure 4a. A 5% modification has been applied to each parameter and the influence on the mechanical strength to pull-out has been measured. Figure 4b shows that two parameters have a major influence on the mechanical strength: the punch radius Rp and the lower die depth Pm.
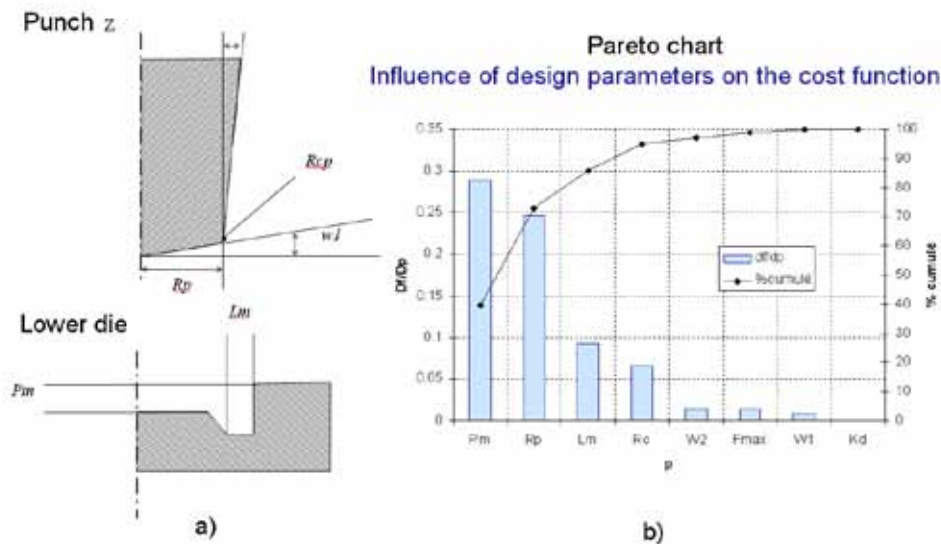

Figure 4: a) Clinching tools geometry and b) Influence of clinching process parameters on the final mechanical strength to pull-out.

5 PROCESS OPTIMIZATION

The numerical problem is to find the minimum of the cost function which represents the practical objective of the optimization. Several methods were attempted using complex derivatives of the cost function (see e. g. [16, 17]). However it is now preferred to use optimization algorithms that require only computation of the cost function. In the following, two examples are presented in order to illustrate the different approaches which are developed in the laboratory.

5.1 Optimization with a single objective

Here the objective is to find the clinching tools geometry that maximizes the final mechanical strength of the clinched component. The sensitivity analysis of section 4 allows us to select two parameters: the punch radius Rp and the lower die depth Pm. Using the MOOPI software, our methodology is summarized in Figure 5.
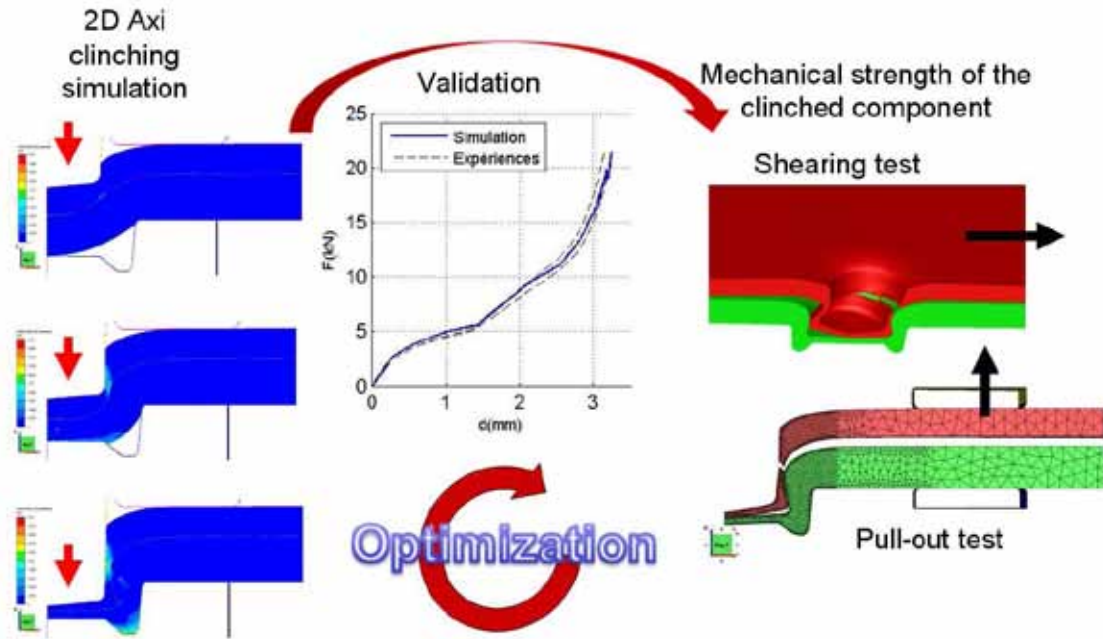

Figure 5 : Optimization of the whole chain of simulation, including the clinching process and the simulation of the shearing and pull-out test.

Table 1 shows the nominal values of the two parameters, the research space and the final optimal values identified by MOOPI.

	Nominal value	Research space	Optimal identified value
Rp (mm)	1.9	[1.6, 2.2]	1.96
Pm (mm)	0	[-0.3, 0.6]	0.16

Table 1 : Nominal values, research space and optimal values associated to the punch radius and the lower tool depth

In Figure 6a it can be seen that damage has been significantly decreased in the upper sheet thanks to the tools geometry modification. Figure 6b shows the response surface associated to the fracture strength to pull-out, that has been maximized. It is interesting to stress that in addition to a higher mechanical strength, the optimal solution is also surrounded by a smooth maximal area, so that a slight perturbation (or variability) of Rp and Pm will not have much
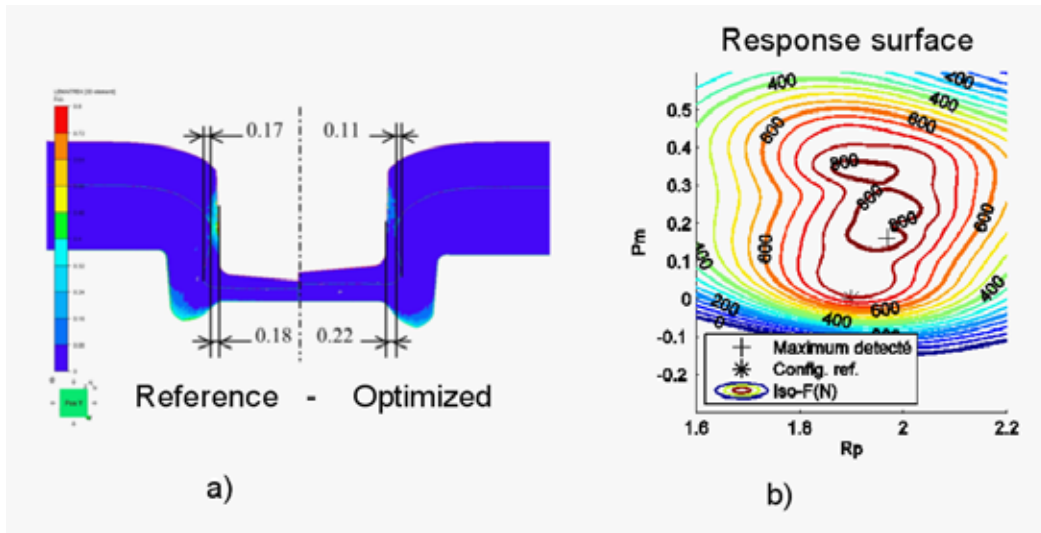
influence on the final mechanical strength.

Figure 6 : a) Map of the final damage field, and b) Response surface associated of the final mechanical strength of the clinched component (* for reference, + for optimized configurations).

Table 2 shows the mechanical strength associated with the reference and optimal configurations. It can be seen that the optimized configuration induces an increase of 13.5% of the mechanical strength to pull-out, and of 42% of the mechanical strength to shearing.

	Mech Strength **Pull-out** (N)	Mech Strength **Shearing** (N)
Reference configuration	737	814
Optimized configuration	840	1193
Benefit (%)	**13.5%**	**42.1%**

Table 2 : Mechanical strengths for a pull-out and shearing test associated with the reference and optimal configurations

5.2 Multi objective optimization

Traditionally, in wire-drawing industry uses the optimization of the drawing force to design wire-drawing dies. The optimum die semi-angle is claimed to be 6°, or more generally is in a range between 4° and 8°. A second objective raises ambiguities, as the risk of ductile fracture should be estimated on a damage criterion. For instance, high-carbon drawn wire may show brittleness either during the drawing process, or at the cabling stage, or during wire service life. Then we have a multi-objective framework, the solution consists in a family of non-dominated solutions that constitute the Pareto optimal set, or the decision space *S*.
The industrial wire drawing process has been simulated following Bobadilla et al [18]. The mechanical analysis of the drawing process is performed by a 2D axi symmetric simulation. Dies are assumed non deformable and the drawing speed is constant. In Figure 7 the mesh

size is 0.5mm and the total nodes number is about 10,000. The wire is long enough to reach the mechanical steady state.
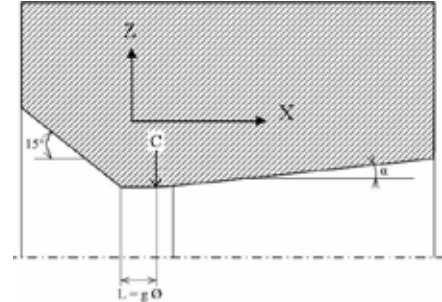

Figure 7 : Wire drawing mesh - Die geometry and corresponding design parameters

The Latham and Cockcroft (L&C) damage criterion is used as one of the objective function:

$$D_{max} = \underset{\Omega}{Max}\left(\int_0^{\varepsilon_f} \frac{max(\sigma_I,0)}{\sigma_{eq}} d\varepsilon_p \right) \qquad (16)$$

Alternatively, the wire drawing force F will be taken as an objective function. Bi-objective optimization (force and damage) will finally be addressed.

The shape parameters describe the geometry of the wire drawing die: reduction ratio R, die semi-angle α and the die length L as illustrated in Figure 7. The land length has no significant impact on the minimization of F or D_{max}. In single pass optimization, reduction ratio cannot be an optimization parameter, which leaves one optimization parameter: the die semi-angle α with values included in the range [1.2°; 22.5°]; this wide range has been selected not to exclude non-conventional solutions.

The selected multi-objective evolutionary algorithm (MOEA) is the Non Sorting Genetic Algorithm, NSGA-II, which is considered one of the most efficient MOEA to find Pareto optimal sets. In order to reduce computational costs, NSGA-II is coupled [19] to a metamodel based on the Meshless Finite Difference Method (MFDM). After initiating the metamodel with a reduced number of individuals, the metamodel is continuously updated during the algorithm iterations. This way, quite accurate Pareto fronts can be obtained by approximately the same number of function evaluations as in the single-objective case.

Optimization provides different optimal die semi-angle (α_{opt}) depending on the objective function. Indeed, an optimal die angle minimizing the non-dimensional drawing stress is found only when friction is non-zero (see Figure 8). On the other hand, no optimal die angle is observed in damage minimization, as the lowest damage is found on the lower bound ($\alpha = 1.2°$ here, see Figure 8). Finally, L&C damage criterion and the non-dimensional wire drawing force have been coupled into a bi-objective approach. The Pareto Optimal Front has been accurately constructed in a single optimization operation, showing these two objective functions to be in conflict. This curve in Figure 9 enables the user to set his priority either on damage or on drawing force. In this case, accepting a 2.1% increase of the drawing force

could save as much as 51% damage, at a die semi-angle $\alpha = 3.46°$. Therefore, damage can be strongly decreased with a slight increase of the reduced drawing force.
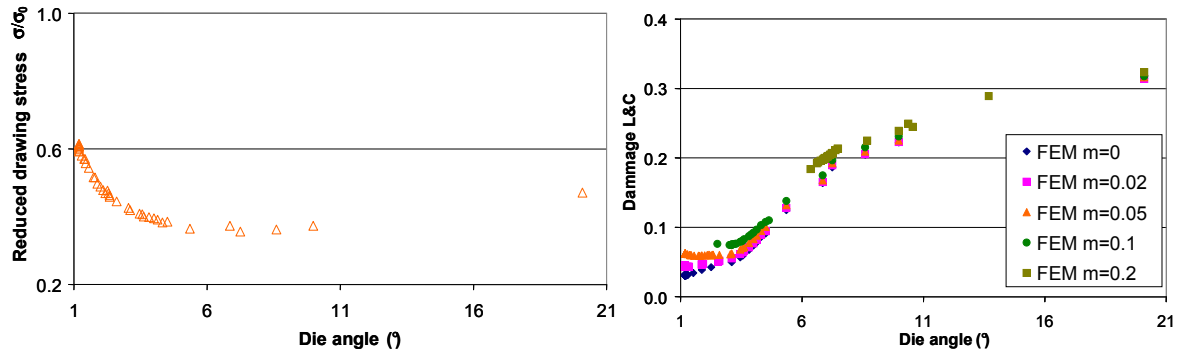

Figure 8 : Wire drawing force (left) and damage (right) versus die angle from a single objective optimization.
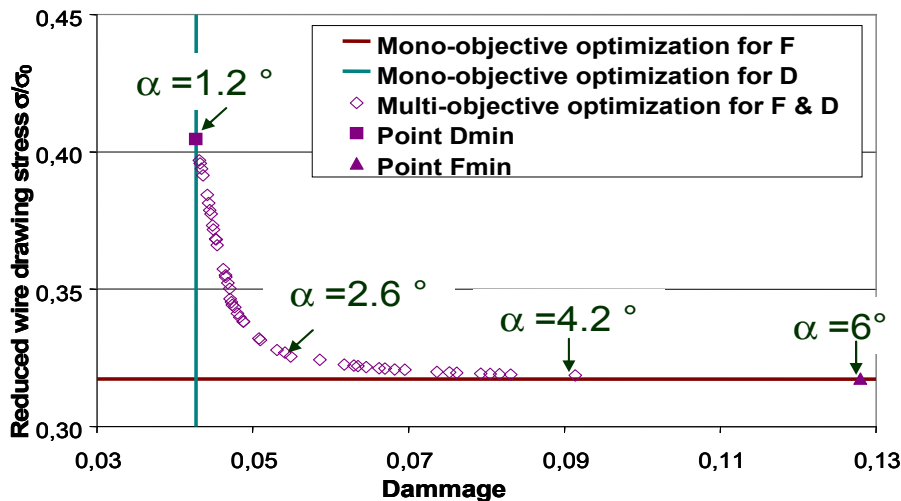

Figure 9 : Pareto front (wire drawing force versus damage) of the multi-objective optimization problem.

6 TOWARD PREDICTION AND OPTIMIZATION OF LOCAL MECHANICAL PROPERTIES

Forged components are recognized for their excellent mechanical strength and fatigue properties. The methodology presented here consists in improving fatigue analyses of forged components by accounting for the forging simulation stage. Kneading rate and grain flow orientation are two consequences of the forging process. Using the FORGE software, grain flow orientation is computed all along the forming process simulation. This grain flow orientation, as well as residual stresses, are input data for predicting fatigue, using an anisotropic extension of the Papadopoulos fatigue criterion. It is based on experimental fatigue results obtained on samples extracted at 0°, 45° and 90° with respect to the grain flow orientation. A numerical modelling is performed at the microscale using the DIGIMICRO

software. These simulations give a better understanding on the influence of elongated particles and cluster of particles on high cycle fatigue mechanisms. A virtual simulation chain is set-up to work on real industrial components. This simulation chain, together with microscale numerical modelling demonstrate the positive influence of the grain flow orientation of forged components on high cycle fatigue properties of industrial parts. The general methodology is schematically illustrated in Figure 10 and the complete description of the work is given in ref. [20].
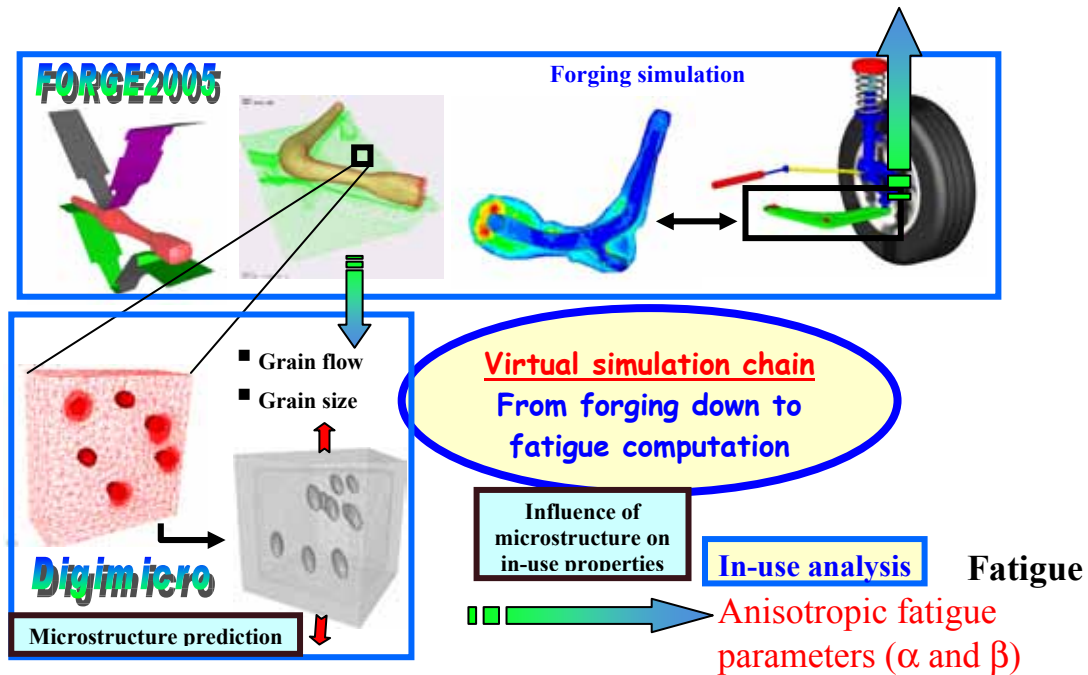

Figure 10 : Prediction and optimization of fatigue for forged components

7 CONCLUSIONS

The basic scientific ingredients were reviewed for accurate simulation of metal forming processes with a finite element computer code. A general software system was presented which will allow the user not only to simulate industrial processes but also to identify material parameters by inverse modeling, to assess the sensitivity of the results to process parameters and to optimize the whole forming sequence. An example of multi scale prediction of fatigue properties of a forged part was given as a first step toward optimization of the final properties of the work-pieces.

REFERENCES

[1] Iwata K., Osakada K. and Fujino S., *Transactions of the ASME*, Ser. B, 94-2, 1972, pp. 697-703.
[2] Cornfield G. C. and Johnson R. H., *J. Iron Steel Inst.*, 211, 1973, p. 567.
[3] Lee C. H. and Kobayashi S*., J. Eng. Ind.*, 95, 1973, p. 865.

[4] Zienkiewicz O. C., and Godbole K., *Int. J. Numer. Meth. Eng.*, 8, 1974, p. 3.

[5] Surdon G. and Chenot J.-L., *Int. J. Numer. Meth. Eng*, 24, 1987, pp. 2107-2117.

[6] Wagoner R. H. and Chenot J.-L., *Metal Forming Analysis*, Cambridge University Press, Cambridge (2001).

[7] Fourment L. and Chenot J.-L., *Computational Plasticity. Fundamentals and Applications*, ed. by Owen D. R. J. et al., Pineridge Press, Swansea, U.K. (1992) 199-212.

[8] Coupez T., Digonnet H. and Ducloux R., *Appl. Math. Model* (2000) **25**:153-175.

[9] Fourment L., Popa S. and Barboza J., *8th Conference On Numerical Methods in Industrial Forming Processes*, Columbus, Ohio, USA, (2004) June

[10] Rey B., Mocellin K. and Fourment L., 8th *European Multigrid Conference EMG 2005*, Scheveningen The Hague, (2005) 27-30 September.

[11] Ramadan M., Fourment L. and Digonnet H., *The 13th International ESAFORM Conference on Material Forming - ESAFORM 2010*, Brescia Italy (2010) April 7-9

[12] Chenot J.- L. and Chastel Y., *J. Mat. proc. Tech.* (1996) **60**:11-18.

[13] Bernacki M., Chastel Y., Coupez T. and Logé R.E., *Scripta Mater.* (2008) **58**:1129-1132.

[14] Gavrus A., Massoni E. and Chenot J.-L., *J. Mat. proc. Tech*. (1996) **60**:447-454.

[15] Jones D. R., Schonlau M. and Welch W. J., *Journal of global optimization* (1998) **13**:455-492.

[16] Fourment L. and Chenot J.-L., *Int. J. Num. Meth. in Engng*. (1996) **39**, 1:33-50.

[17] Fourment L., Balan T. and Chenot J.-L*., Int. J. Num. Meth. in Engng*. (1996) **39**, 1:51-66.

[18] Bobadilla C., Persem N. and Foissey S., *Published by AIP Conf. Proc*., (2007) **907**:535-540.

[19] Ejday M. and Fourment L., *Int. J. Mater. Form*. (2010) **3**-1:5-8.

[20] Milesi M., Chastel Y., Hachem E., Bernacki M., Loge R.E., and Bouchard P.O., *Mater. Sci. Engng. A* (2010) **527**, 18-19:4654-4663.